

Properties of High T_c Superconducting Quantum Interference Device Microscope with High μ -Metal Needle

Saburo TANAKA, Kazuka MATSUDA, Osamu YAMAZAKI, Miyuki NATSUME, Hajime OTA and Takahiro MIZOGUCHI

Department of Ecological Engineering, Toyohashi University of Technology,
1-1 Hibarigaoka, Tempaku-cho, Toyohashi, Aichi 441-8580, Japan

(Received January 31, 2001; accepted for publication March 14, 2001)

A new type of superconducting interference device (SQUID) microscope was designed and fabricated. A direct-coupled SQUID magnetometer with a high μ -metal needle was used and the substrate was machined to create a dimple for the needle at the center of the pick-up loop. One end of the needle penetrated through the superconducting pick-up loop in a vacuum; the needle was fixed in the vacuum window with the other end at room temperature in the outside atmosphere. As a demonstration, a laser printed output was scanned by the microscope. Line bars with a line width of $100\ \mu\text{m}$ and a spacing between lines of $200\ \mu\text{m}$ were clearly imaged.

KEYWORDS: high T_c SQUID, microscope, flux guide

In recent years superconducting interference devices (SQUIDs) have been used in a wide variety of applications due to their superior magnetic field sensitivity. In particular, SQUID microscopes have become a powerful tool for the investigation of flux dynamics and other studies in physics.^{1–6} For a low T_c SQUID, a small transfer coil was developed and connected to the SQUID.^{3,4} However, for a high T_c SQUID, there is no technology to transfer a small magnetic field from a small area to the SQUID. Therefore, the high T_c SQUID must be sufficiently small and the separation of the SQUID and the sample must be as small as possible. Some groups have proposed a high T_c SQUID microscope using a high μ -metal tip or needle to solve the above-mentioned problems.^{7–10} The advantage of this system is that magnetization of the sample by the modulation coil of the SQUID can be avoided, because the coil is far enough from the sample. We have designed and fabricated a new type of high T_c microscope using a fine flux guide. One end of the flux guide penetrates through the pick-up loop of the 77 K SQUID; the needle was held by the window with the other end sharpened and at room temperature. A system in which a room temperature flux guide penetrates the SQUID pick-up loop has not been reported on to date. We present a design based on a computer simulation of the magnetic field distribution and the results of the microscope.

Figure 1 shows the schematic drawing of a direct coupled dc SQUID. It was made of a 200 nm-thick $\text{YBa}_2\text{Cu}_3\text{O}_{7-y}$ (YBCO) thin film on a $500\ \mu\text{m}$ -thick SrTiO_3 substrate by sputtering. The junctions utilized in the SQUID are a 30-degree bi-crystal type. The inductance of the SQUID and the pick-up loop are 40 pH and 3 nH from calculations, respectively. The outer and inner diagonal dimensions of the pick-up loop are $\phi 6.4\ \text{mm}$ and $\phi 2.2\ \text{mm}$, respectively. The substrate at the center of the pick-up loop was machined so that a 100–200 μm deep-dimple was created for the needle space. It was not a through-hole but a dimple because the substrate was fragile.

A schematic cross-sectional view of the microscope is shown in Fig. 2. Most of the parts of the cryostat are made of G-10 fiberglass and Delrin.⁵ The cryostat contains a liquid N_2 copper reservoir, having a volume of 0.8 liters. The inside of the cryostat can be evacuated up to the order of

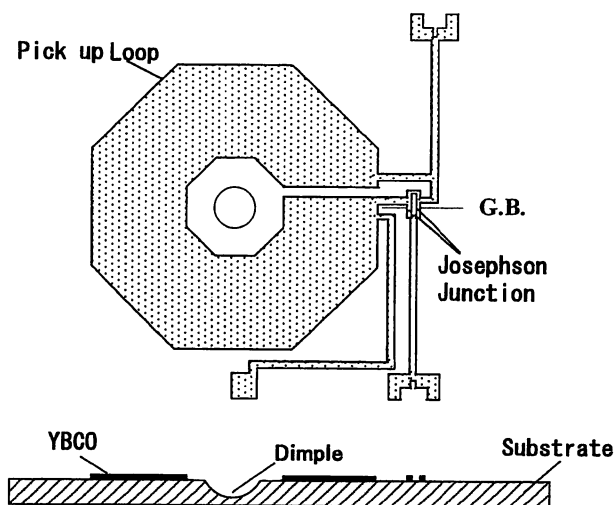


Fig. 1. Schematic drawing of a directly coupled dc SQUID. The SQUID inductance is 40 pH in the calculation. The outer and inner diagonal dimensions of the pick-up loop are $\phi 6.4\ \text{mm}$ and $\phi 2.2\ \text{mm}$, respectively. The substrate at the center of the pick-up loop was machined so that a 100–200 μm deep-dimple is created for the needle space.

$10^{-3}\ \text{Pa}$ by a vacuum pump and sealed off by an o-ring valve. The SQUID chip was attached to the top of a $\phi 12$ sapphire rod with GE varnish, which was thermally anchored with the liquid N_2 reservoir. The SQUID was 50 mm away from the metallic reservoir. A 6-turn modulation coil and a heater were installed in the upper end of the sapphire rod. A copper wire step-up transformer was glued tightly to the top of the copper reservoir. The electrical contacts to the SQUID chip were made by applying conductive silver paint to the bonding pads and the side of the SQUID chip.

A needle made of a high μ -metal was set at the center of the pick-up loop. The length of the needle was 7 mm; its cross-section at the bottom was a $300\ \mu\text{m} \times 300\ \mu\text{m}$ square shape. The top of the needle was filed so that it had a sharp edge. The diameter of the top edge was $50\ \mu\text{m}$ from microscope observation. The needle penetrated a vacuum window through a hole. About $100\ \mu\text{m}$ from the top of the needle was outside of the window. The hole was sealed with a silicone rubber glue after penetration. The distance between the needle and the pick-up loop was adjustable by turning three

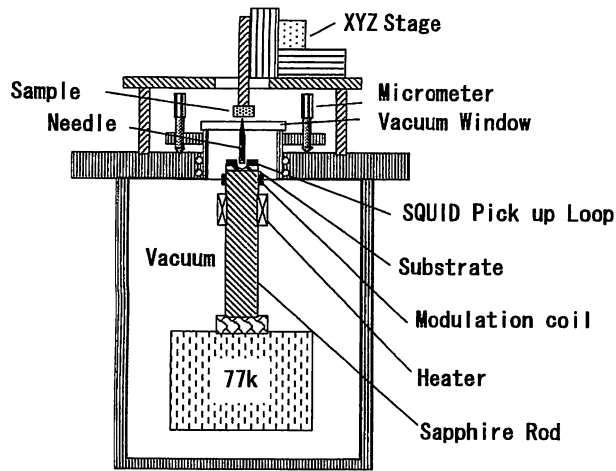


Fig. 2. Schematic cross-sectional view of the SQUID microscope. The SQUID chip was on the top of a sapphire rod, which was thermally anchored with a liquid N_2 reservoir. A needle made of a high μ -metal was set at the center of the pick-up loop. The length of the needle was 7 mm. The needle penetrated the vacuum window through a hole. Approximately $100\ \mu\text{m}$ from the tip of the needle was outside of the window. The hole was sealed with silicone rubber glue after penetration.

micrometers.

A home-made XYZ translation stage was placed on the top plate of the cryostat. The stage was made of an aluminum alloy and steel and driven by an ultrasonic linear motor. The minimum step size is $0.5\ \mu\text{m}$. The translation stage is controlled by a personal computer using signals from positioning sensors. The maximum scan range is $6 \times 6\ \text{mm}^2$.

Firstly, we investigated the feasibility of this method using computer simulations. The three-dimensional FEED electrodynamic simulation program, Maxwell (supplied by Ansoft Japan), was used. We selected a perfect conductor as the material for the pick-up loop instead of a superconductor because there was no superconducting material in the library. The permeability of the needle μ_r was selected as 60000. The details of the simulation parameters and dimensions are shown in Fig. 3. One set of small field coils with a separation of $600\ \mu\text{m}$, which generates a magnetic field of $33.3\ \text{A/m}$ was positioned above the pick-up loop. The relative position of the set of coils and the pick-up loop was varied by steps of $150\ \mu\text{m}$ in this simulation. The field calculation at the center of the pick-up coil was performed at each position. Figure 4 shows the results of the simulation. In the case of (a) the needle penetrates through the loop. The bottom of the needle is $500\ \mu\text{m}$ below the film in this case. In the case of (b) the needle is at the same level as the loop. In the case of (c) the needle is above the loop with a space of $500\ \mu\text{m}$. Two peaks, one at the position of each field coil, were observed in all the cases. However, the field density in the case of (a) is the largest and one order of magnitude larger than that in the case of (c). This suggests that the penetration of the needle through the pick-up loop is essential to obtaining a higher sensitivity.

The performance of the direct-coupled SQUID magnetometer was investigated. A needle was positioned at the center of the pick-up loop. The needle was brought into contact once with the bottom of the dimple of the substrate by adjusting the micrometer and it was then lifted up a little bit above the bottom for thermal isolation.

The SQUID was driven by a flux-locked loop with a flux

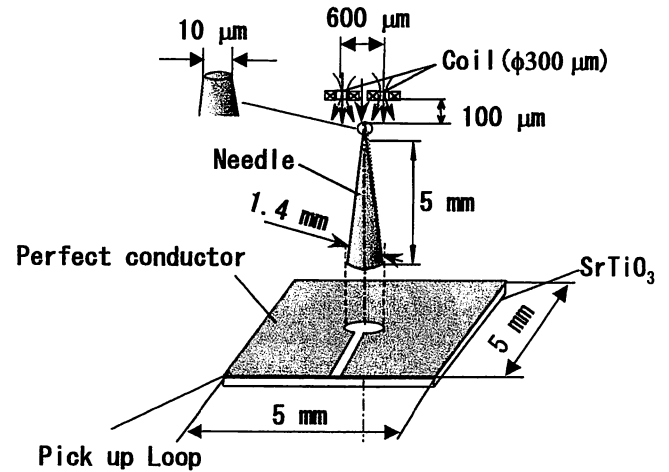


Fig. 3. Model of the simulation. One set of small field coils with a separation of $600\ \mu\text{m}$, which generated a magnetic field of $33.3\ \text{A/m}$ was positioned above the pick-up loop. The relative position of the set of coils and the pick-up loop was varied by a step of $150\ \mu\text{m}$ in this simulation. The separation between the top of the needle and the coil was $100\ \mu\text{m}$ and constant.

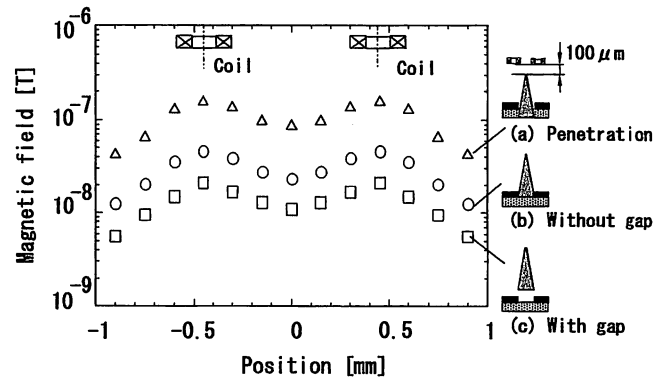


Fig. 4. Simulation results. Two peaks, one at the position of each field coil, were observed in all the cases. The field density in the case of (a) is the largest and one order of magnitude larger than that in the case of (c).

modulation frequency of $256\ \text{kHz}$. The output signal from the SQUID was amplified by double transformers, one at $77\ \text{K}$ and the other at room temperature. The R_f/M_f is $0.5\ \text{V}/\phi_0$, where R_f is the feedback resistance and M_f is the mutual inductance between the SQUID magnetometer and the modulation coil. All of the measurements were performed in a magnetically shielded room, which had a shielding factor of $-50\ \text{dB}$. A small one-turn coil with a radius of $1\ \text{mm}$ was prepared and put on the top end of the needle to measure the local effective area at the edge of the needle. A small coil rather than a large coil was used to avoid having the field from the coil couple directly to the pick-up loop of the SQUID. A sinusoidal current of $1\ \text{mA}_{\text{p-p}}$ with a frequency of $100\ \text{Hz}$ was used. Then we found that the effective area $A_{\text{eff-needle}}$ of the magnetometer was $540\ \text{mm}^2$. This value corresponds to a small SQUID with a washer size of about $15\ \mu\text{m} \times 15\ \mu\text{m}$.²⁾ The flux noise of the magnetometer was measured. While the flux noise $S_\phi^{1/2}(f)$ without needle was $28\ \mu\phi_0/\text{Hz}^{1/2}$ at $100\ \text{Hz}$ and $27\ \mu\phi_0/\text{Hz}^{1/2}$ in the white noise region, the noise with needle was $80\ \mu\phi_0/\text{Hz}^{1/2}$ at $100\ \text{Hz}$ and $36\ \mu\phi_0/\text{Hz}^{1/2}$ in the white noise region. Excess $1/f$ flux noise, which may be generated by the thermal activated hopping of vortices trapped

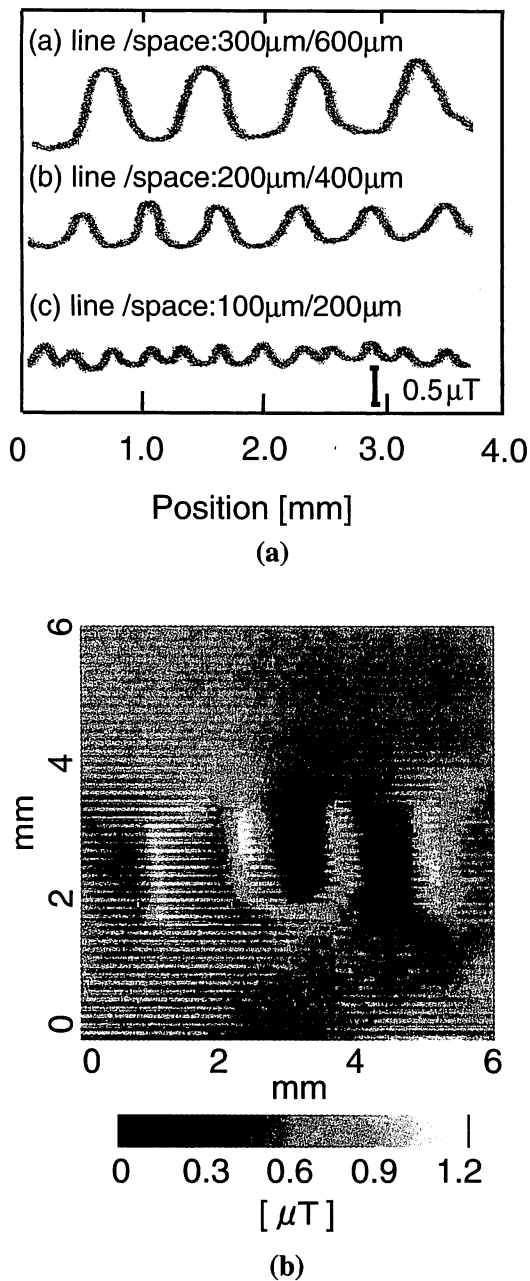


Fig. 5. (a): The output signal of the SQUID when laser-printed bar patterns are scanned. The finest pattern we prepared was a line width of $100\ \mu\text{m}$ and a spacing between lines of $200\ \mu\text{m}$. (b): Two dimensional magnetic field image of the printed pattern of the characters "TUT".

during cooldown was observed in the case with needle. However, since the optimal bias current was not changed in the measurements with and without the needle, the trapping was not significant.

Laser printed outputs were used as a sample to test the microscope. Laser printer ink contains ferromagnetic particles and therefore it is easy to generate a bar line. The finest pattern we prepared was a line width of $100\ \mu\text{m}$ and a spacing between lines of $200\ \mu\text{m}$. This pattern was restricted by the resolution of the laser printer. The samples were moved in the direction that the needle crosses the bar lines. The XY translation stage was not used in this experiment, however, a pattern was made from a thin string drawn by a miniature induction motor installed outside of the magnetically shielded

room. The velocity of the scanning was $620\ \mu\text{m/s}$. The surface of the sample was brought into contact with the end of the needle during the scan. Figure 5(a) shows the output signal of the SQUID. The signal was measured through a low pass filter of 5 kHz. All of the patterns were clearly observed. The peak-peak value of the signal that corresponds to the line was about $0.15\ \mu\text{T}$. Therefore this system has at least a resolution of $\text{line/space} = 100\ \mu\text{m}/200\ \mu\text{m}$.

Then we raster scanned the printed output pattern of the characters "TUT" using the XYZ translation stage. It took 150 s to scan the $6\ \text{mm} \times 6\ \text{mm}$ area. The signals in the bandwidth range of 0.8 Hz to 5 kHz were measured to eliminate the background field. The step sizes are $2\ \mu\text{m}$ in the X direction and $20\ \mu\text{m}$ in the Y direction. The separation between the sample and the end of the needle was adjusted to be about $100\ \mu\text{m}$ to avoid the friction between the sample and the needle edge. Figure 5(b) shows the obtained image. Inhomogeneity of the line to space ratio is due to the quality of the laser printed patterns. The image was in good agreement with the sample.

In conclusion, we have designed and constructed a new type of magnetic microscope using a high- T_c SQUID with a high- μ metal room temperature needle. One end of the needle penetrated a superconducting pick-up loop in a vacuum; the needle was fixed in the vacuum window with the other end at room temperature in the outside atmosphere. Using an FEED electro-dynamic simulation, it was found that when the needle penetrated the superconducting loop, the magnetic field density at the loop was one order of magnitude larger than that of the case of no penetration. Therefore the substrate of a direct-coupled SQUID magnetometer was machined to create a dimple at the center of the pick-up loop to provide room for the needle. Laser printed output was scanned by the microscope. Line bars with a line width of $100\ \mu\text{m}$ and a spacing between lines of $200\ \mu\text{m}$ were clearly imaged. We think that the space resolution can be improved by using a sharper needle edge.

This work was partially supported by a Grant-in-Aid for Scientific Research in Priority Area (A) from the Ministry of Education, Culture, Sports, Science and Technology.

- 1) R. C. Black, A. Mathai, F. C. Wellstood, E. Dantsker, A. H. Miklich, D. T. Nemeth, J. J. Kingston and J. Clarke: *Appl. Phys. Lett.* **62** (1993) 2128.
- 2) T. S. Lee, E. Dantsker and J. Clarke: *Rev. Sci. Instrum.* **67** (1996) 4208.
- 3) J. R. Kirtley, M. B. Ketchen, K. G. Stawiasz, J. Z. Sun, W. J. Gallagher, S. H. Blanton and S. J. Wind: *Appl. Phys. Lett.* **66** (1995) 1138.
- 4) T. Morooka, S. Nakayama, A. Odawara, M. Ikeda, S. Tanaka and K. Chinone: *IEEE Trans. Appl. Supercond.* **9** (1999) 3491.
- 5) S. Tanaka, O. Yamazaki, R. Shimizu and Y. Saito: *Supercond. Sci. Technol.* **12** (1999) 809.
- 6) E. F. Fleet, S. Chatrathorn, F. C. Wellstood and L. A. Knauss: *IEEE Trans. Appl. Supercond.* **9** (1999) 4103.
- 7) P. Pitzius, V. Dworak and U. Hartmann: *Ext. Abstr. 6th Int. Supercond. Electronics Conf. (ISEC'97)*, 1997, Vol. 3, p. 395.
- 8) Y. Tavrinn and M. Seigel: *Appl. Supercond.* **1** (1998) 719.
- 9) T. Nagaishi, K. Minamimura and H. Itozaki: to be published in *IEEE Trans. Appl. Supercond.* (2001).
- 10) S. A. Gudoshnikov, Y. V. Deryuzhkina, P. E. Rudenchik, Y. S. Sintmov, S. I. Bondarenko, A. A. Shablo, P. P. Pavlov, A. S. Kalabukhov, O. V. Snigirev and P. Seidel: to be published in *IEEE Trans. Appl. Supercond.* (2001).